



Mitochondrial superoxide disrupts the metabolic and epigenetic landscape of CD4⁺ and CD8⁺ T-lymphocytes

C.M. Moshfegh^a, C.W. Collins^a, V. Gunda^b, A. Vasanthakumar^c, J.Z. Cao^c, P.K. Singh^b, L.A. Godley^c, Adam J. Case^{a,*}

^a Department of Cellular and Integrative Physiology, University of Nebraska Medical Center, Omaha, NE, United States

^b The Eppley Institute for Research in Cancer and Allied Diseases, University of Nebraska Medical Center, Omaha, NE, United States

^c Section of Hematology/Oncology, Department of Medicine, The University of Chicago Medicine Comprehensive Cancer Center, Chicago, IL, United States

ARTICLE INFO

Keywords:

Redox
Oxidative stress
Manganese superoxide dismutase
Immune
Adaptive immunity
Cytokines
Proliferation
Apoptosis
Metabolism
Methylation
Hydroxymethylation

ABSTRACT

While the role of mitochondrial metabolism in controlling T-lymphocyte activation and function is becoming more clear, the specifics of how mitochondrial redox signaling contributes to T-lymphocyte regulation remains elusive. Here, we examined the global effects of elevated mitochondrial superoxide ($O_2^{\cdot-}$) on T-lymphocyte activation using a novel model of inducible manganese superoxide dismutase (MnSOD) knock-out. Loss of MnSOD led to specific increases in mitochondrial $O_2^{\cdot-}$ with no evident changes in hydrogen peroxide (H_2O_2), peroxynitrite ($ONOO^-$), or copper/zinc superoxide dismutase (CuZnSOD) levels. Unexpectedly, both mitochondrial and glycolytic metabolism showed significant reductions in baseline, maximal capacities, and ATP production with increased mitochondrial $O_2^{\cdot-}$ levels. MnSOD knock-out T-lymphocytes demonstrated aberrant activation including widespread dysregulation in cytokine production and increased cellular apoptosis. Interestingly, an elevated proliferative signature defined by significant upregulation of cell cycle regulatory genes was also evident in MnSOD knock-out T-lymphocytes, but these cells did not show accelerated proliferative rates. Global disruption in T-lymphocyte DNA methylation and hydroxymethylation was also observed with increased mitochondrial $O_2^{\cdot-}$, which was correlated to alterations in intracellular metabolite pools linked to the methionine cycle. Together, these results demonstrate a mitochondrial redox and metabolic couple that when disrupted may alter cellular processes necessary for proper T-lymphocyte activation.

1. Introduction

Modern day life evolved to exist in an oxidative environment, which has forced organisms to adapt to reactive oxygen-based species (ROS) [1]. These volatile species are often products of electron transfer to molecular oxygen, and cells have developed complex antioxidant systems to prevent uncontrolled damage by these molecules. With the acquisition and passage of precious electrons at the heart of cellular life, it is no surprise that life eventually evolved to limit energy waste and utilize ROS in normal cellular processes. However, a fine line exists between this so called normal redox signaling and uncontrolled oxidative stress that still remains unclear [2].

Redox signaling in the adaptive immune system has particularly remained elusive. Compared to the well-described oxidative burst of innate immune cells, much less is known regarding the role of ROS in lymphocytes. Early studies identified a necessary role for NADPH oxidase (NOX)-driven superoxide ($O_2^{\cdot-}$) in the activation of T-

lymphocytes, but the specific NOX isoform and downstream effects of this $O_2^{\cdot-}$ were not fully elucidated [3]. Since this time, the vast majority of studies have focused on NOX-derived redox signaling and redox-sensitive transcription factors in T-lymphocytes [4]. Due to this, the role of mitochondrial-derived redox signaling continues to be enigmatic.

Mitochondria are critical metabolic organelles in T-lymphocytes, and are necessary for T-lymphocyte activation and differentiation [5–7]. This concept is a recent paradigm shift from the antiquated view that T-lymphocytes exclusively utilize aerobic glycolysis for their metabolic demands. Additionally, the incorporation of these organelles into a working model of T-lymphocyte function has raised new questions regarding how oxygen demand, metabolism, epigenetic regulation, and redox signaling affect these adaptive immune cells. Recent studies have attempted to examine the role of mitochondrial-derived ROS in T-lymphocytes [8,9]. However, these studies manipulated the mitochondrial electron transfer chain to elicit changes in the

* Corresponding author. Department of Cellular and Integrative Physiology, 985850 Nebraska Medical Center, Omaha, NE 68198-5850, USA.
E-mail address: adam.case@unmc.edu (A.J. Case).

<https://doi.org/10.1016/j.redox.2019.101141>

Received 4 January 2019; Received in revised form 5 February 2019; Accepted 11 February 2019

Available online 21 February 2019

2213-2317/ © 2019 The Authors. Published by Elsevier B.V. This is an open access article under the CC BY-NC-ND license (<http://creativecommons.org/licenses/by-nc-nd/4.0/>).

mitochondrial redox environment, which convolutes the interpretation of the results in regards to redox signaling versus metabolic function. To avoid this, we previously developed a model of T-lymphocyte-specific increased steady-state mitochondrial $O_2^{\cdot-}$ by deleting the sole mitochondrial $O_2^{\cdot-}$ -removal enzyme manganese superoxide dismutase (MnSOD; encoded by the *Sod2* gene). Using this model along with neonatal mitochondrial antioxidant supplementation, we showed that a proper balance of mitochondrial $O_2^{\cdot-}$ was required for T-lymphocyte development, as mice lacking MnSOD in T-lymphocytes or that were over-supplemented with mitochondrial antioxidants displayed significant immunosuppression [10]. While this study identified a role of mitochondrial $O_2^{\cdot-}$ in T-lymphocyte development, the question of how mitochondrial $O_2^{\cdot-}$ affects mature T-lymphocytes in a fully developed organism remained unanswered.

Herein, we set out to examine how uncontrolled endogenous mitochondrial $O_2^{\cdot-}$ affects T-lymphocyte activation and function in mature $CD4^+$ and $CD8^+$ T-lymphocytes utilizing an inducible MnSOD knock-out strategy. We show that mitochondrial $O_2^{\cdot-}$ has profound effects on cellular metabolism, strengthening the hypothesis that redox and metabolism are inseparable entities. Additionally, while we identified that increased mitochondrial $O_2^{\cdot-}$ leads to increased apoptosis in T-lymphocytes, we unexpectedly observed that MnSOD knock-out T-lymphocytes showed no deficits in their proliferative capacity. Moreover, MnSOD knock-out T-lymphocytes displayed a stronger replicative gene expression signature compared to controls even in their naïve state. Last, we elucidated that mitochondrial $O_2^{\cdot-}$ dysregulated pan-cytokine and chemokine expression, which may be due to a global disruption of the metabolic-epigenetic landscape by this specific sub-cellular ROS.

2. Materials and methods

Mice. All experiments were performed using 8-12 week-old male mice of a C57BL/6J background. Examination of sex differences or hormonal effects were not aims of the study described herein. Our development of tamoxifen-inducible conditional MnSOD knockout mice has been previously described [11]. Briefly, mice possessing loxP elements flanking exon 3 of the *Sod2* gene locus (i.e. B6.Cg-*Sod2*^{tm1Lox}) were crossed to mice possessing a ROSA26 promoter driven tamoxifen-inducible cre-recombinase (i.e. B6.129-Gt(ROSA)26^{Sortm1(cre/ERT2)Tvj/J}) to the F3 generation. This allows for 100% homozygous *Sod2* loxP progeny with 50% either Cre^{+/-} (knockouts) or Cre^{-/-} (controls). ROSA26-driven inducible cre-recombinase expression was utilized due to a lack of specific CD4 and CD8 inducible cre-recombinase mouse strains at the initiation of these studies. All studies were performed on T-lymphocytes *ex vivo* to eliminate effects of non-target cell MnSOD knockout. Mice were housed with standard corn cob bedding, paper nesting material, and given access to standard chow (Teklad Laboratory Diet #7012, Harlan Laboratories, Madison, WI) and water ad libitum. Littermates, independent of genotype, were group housed to no more than 5 mice per cage to eliminate social isolation stress, and to ensure comparable living conditions among experimental groups. To induce MnSOD knockout, all mice were treated daily with tamoxifen (Sigma-Aldrich #T5648, St. Louis, MO) for 5 days beginning at approximately 8–9 weeks of age. Tamoxifen was resuspended at 20 mg/mL in sunflower seed oil (Sigma-Aldrich #S5007, St. Louis, MO) and injected intraperitoneally at 150 mg/kg/day. Injections occurred in home cages, and mice were sacrificed two weeks following the last tamoxifen injection to allow remnant MnSOD protein to degrade. Mice were euthanized by pentobarbital overdose (150 mg/kg, Fatal Plus, Vortech Pharmaceuticals, Dearborn, MI) administered intraperitoneally. All mice were sacrificed between 0700 and 0900 Central Standard Time to eliminate circadian rhythm effects on T-lymphocyte function. Mice were randomized prior to the start of all experiments, and when possible, experimenters were blinded to the genotypes of mice until the completion of the study. All procedures were reviewed and approved by

the University of Nebraska Medical Center Institutional Animal Care and Use Committee.

2.1. T-lymphocyte isolation and culture

T-lymphocytes were isolated and cultured as previously described [12]. Briefly, splenic $CD4^+$ and $CD8^+$ T-lymphocytes were negatively selected using the EasySep Mouse $CD4^+$ T-Cell Isolation Kit (StemCell Technologies #19852, Vancouver, BC) or $CD8^+$ T-Cell Isolation Kit (StemCell Technologies # 19853, Vancouver, BC), respectively. The purity of the respective lymphocyte populations was randomly quality controlled and assessed by flow cytometry at > 90%. Additionally, CD62L and CD44 staining demonstrate > 90% are in the naïve state after isolation. Live cells (as assessed by a Bio-Rad TC20 Automated Cell Counter using trypan blue exclusion) were seeded on 24 or 96-well culture plates at 250,000 cells/cm² with media depths of 0.3125 cm to ensure equivalent oxygen diffusion. T-lymphocytes were activated in a non-antigenic T-lymphocyte receptor manner by the addition of CD3/CD8 mouse Dynabeads (Thermo Fisher #11453D, Waltham, MA) in a 1:1 ratio with cells. Cells or culture media were utilized for experiments at 96 h post activation unless otherwise stated.

RNA extraction, cDNA production, and quantitative real-time RT-PCR. Assessment of mRNA levels was performed as previously described [13]. Briefly, total RNA was extracted from purified T-lymphocytes using the RNeasy mini kit (Qiagen # 74104, Valencia, CA) according to the manufacturer's protocol. Concentration of RNA was determined spectrophotometrically using a Nanodrop 2000 Spectrophotometer (Fisher Thermo Scientific, Waltham, MA). The high capacity cDNA archive kit (Applied Biosystems #4368813, Grand Island, NY) was used to obtain cDNA from total RNA. Generated cDNA was then subjected to SYBR green (Applied Biosystems #4385612, Grand Island, NY) quantitative real-time PCR with primers specific (Supplemental Table 1) to the coding sequence of the respective genes. PCR product specificity was determined by thermal dissociation. A threshold in the linear range of PCR amplification was selected and the cycle threshold (Ct) determined. Ct values of the various transcripts were then normalized to the Ct values of the 18s loading control (ΔCt), and then these ΔCt values were normalized relative to the control sample ($\Delta\Delta Ct$). Because each cycle in PCR equates to a 2-fold difference in relative abundance, the differences ($\Delta\Delta Ct$) are transformed and expressed as fold changes via equation $2^{-\Delta\Delta Ct}$.

2.2. Western blot analysis

Western blotting for the quantification of proteins was performed as previously described [14]. Briefly, whole cell soluble lysate (30 μ g) was separated by SDS-PAGE and transferred to a nitrocellulose membrane. Membranes were incubated with antibodies directed against MnSOD (1:2000 dilution, Abcam #ab13533, Cambridge, MA), CuZnSOD (1:1000 dilution, Thermo Fisher #MA1105, Waltham, MA), or actin (1:1000 dilution, Sigma Aldrich #A2066, St. Louis, MO) followed by horseradish peroxidase (HRP)-conjugated secondary antibodies (1:10,000, Thermo Fisher #31460, Waltham, MA). Densitometric analysis of band intensity was determined using ImageJ analysis software.

2.3. Sod activity

Activity assays were performed as previously described [10]. Briefly, whole cell soluble lysate (100 μ g) was separated by non-denaturing polyacrylamide gels. Sod activity was assessed by the ability to inhibit the reduction of nitro blue tetrazolium by riboflavin-generated $O_2^{\cdot-}$. CuZnSOD and MnSOD activities are discriminated on the basis of size and gel migration. Densitometric analysis of band intensity was determined using ImageJ analysis software.

2.4. Electron paramagnetic resonance (EPR)

EPR spectroscopy was performed as previously described [12]. Briefly, T-lymphocytes were incubated for 30 min at 37 °C with the cell-permeable O₂^{•-}-sensitive spin probe 1-hydroxy-3-methoxycarbonyl-2,2,5,5-tetramethylpyrrolidine (CMH, 200 μmol/L, Noxygen Science Transfer and Diagnostics, Elzach, Germany) in a Krebs-HEPES buffer (pH 7.4) containing (in mmol/L): 99 NaCl, 4.69 KCl, 2.5 CaCl₂, 1.2 MgSO₄, 25 NaHCO₃, 1.03 KH₂PO₄, 5.6 D-glucose, 20 HEPES, and supplemented with the metal chelators DETC (5 μM) and deferoxamine (25 μM). Cells were analyzed using a Bruker e-scan EPR spectrometer. The following EPR settings were used: field sweep width, 60.0 G; microwave frequency, 9.75 kHz; microwave power, 21.90 mW; modulation amplitude, 2.37 G; conversion time, 10.24 ms; time constant, 40.96 ms.

2.5. Flow cytometric redox assessment

Total and mitochondrial-specific assessment of specific redox species was performed as previously described [12]. Briefly, cells were stained with 10 μM dihydroethidium (DHE; O₂^{•-}-sensitive total cellular probe, VWR #101447-534, Chicago, IL), 1 μM MitoSOX Red (O₂^{•-}-sensitive mitochondrial-localized probe, Thermo Fisher Scientific #M36008, Waltham, MA), 10 μM PY1 (H₂O₂ and ONOO⁻-sensitive total cellular probe, Sigma Aldrich #SML0676, St. Louis, MO), or 1 μM MitoPY1 (H₂O₂ and ONOO⁻-sensitive mitochondrial-localized probe, Sigma Aldrich #SML0734, St. Louis, MO) for 30 min at 37 °C. Cells were analyzed on a LSRII flow cytometer at 488/610 nm ex/em for DHE and MitoSOX and 488/510 nm ex/em for PY1 and MitoPY1.

2.6. Mitochondrial and glycolytic bioenergetics analysis

Mitochondrial bioenergetics assessment was performed as previously described [12]. Briefly, oxygen consumption rate and extracellular acidification rate were assessed using a Seahorse Bioscience XFp extracellular flux analyzer. Cells were plated on Cell-Tak (Corning #354240, Corning, NY) treated plates designed for the XFp analyzer at 200,000 live cells (assessed by trypan blue exclusion) per well in bicarbonate-free basal media supplemented with 11 mM D-glucose, 1 mM sodium pyruvate, and 1X GlutaMAX (Thermo Fisher #35050061, Waltham, MA). Mitochondrial function was assessed using the Seahorse Bioscience Cell Mito Stress Test (Agilent #103015-100, Santa Clara, CA) with the following optimized drug concentrations: 1 μM oligomycin, 1 μM FCCP, and 10 μM rotenone/antimycin A. Glycolytic function was assessed using the Seahorse Bioscience Cell Glycolysis Stress Test (Agilent #103017-100, Santa Clara, CA) with the following optimized drug concentrations: 10 mM D-glucose, 1 μM oligomycin, 50 mM 2-deoxyglucose. Cells from one mouse were run on a single plate in technical triplicates; repeated biological replicate plates were run and data pooled for analysis using Seahorse Wave software.

2.7. Apoptosis, proliferation, and cell cycle

All assays were performed as previously described [13]. For apoptosis analysis, the Alexa Fluor 488 Annexin V/Dead Cell Apoptosis Kit (Life Technologies #V13241, Grand Island, NY) was used as per manufacturer's instructions. For proliferation, carboxyfluorescein succinimidyl ester (CFSE, Sigma Aldrich #21888, St. Louis, MO) was added to cells at time of isolation prior to plating for activation. For cell cycle analysis, T-lymphocytes were resuspended for 20 min in Krishan cell cycle buffer, which consists of 0.05 mg/mL propidium iodide (PI; Sigma-Aldrich #P4170, St. Louis, MO), 0.10% sodium citrate (Fisher Thermo Scientific #BP327, Waltham, MA), 0.03% nonidet P-40 (NP-40; Amresco #E109, Solon, OH), and 0.02 mg/mL RNaseA (Invitrogen #12091-021, Grand Island, NY). All analyses were run on a LSRII flow cytometer and quantified using FlowJo or ModFit cytometric analysis

software.

2.8. Cytokine analysis

Secreted cytokines were assessed by two different methods. At 48 and 96 h post-activation, cell media from T-lymphocyte cultures was analyzed using the mouse Th1/Th2/Th17 cytometric bead array (BD Biosciences #560485, San Jose, CA) as per manufacturer's instructions. Analysis beads were analyzed on a LSRII flow cytometer for quantification of specific cytokines. At 96 h post-activation, cell media was also analyzed using a Meso Scale Discovery 35 U-Plex Mouse Biomarker Group (#K15083K-1, Rockville, MD). Samples were analyzed using a Meso Scale QuickPlex SQ 120, and normalized to cell number.

2.9. Global 5-methylcytosine and 5-hydroxymethylcytosine analysis

Assessment of these epigenetic markers was performed as previously described [15,16]. Briefly, 1 μg of total cellular DNA was first denatured by heating at 100 °C for 3 min and then chilling on ice. After adding a 1/10 volume of 0.1 M ammonium acetate (pH 5.3) and 2 units of nuclease P1, the mixture was incubated at 45 °C for 2 h. A 1/10 volume of 1 M ammonium bicarbonate and 0.002 unit of venom phosphodiesterase I were subsequently added to the mixture, and the incubation was continued at 37 °C for 2 h. Next, 0.5 units of alkaline phosphatase were added, and the mixture was incubated at 37 °C for 1 h. The resultant digestion was then separate by mass spectrometric analysis using an Agilent Zorbax-26 4.6 mm × 50 mm, 3.5 μm particle column at the proteomics core laboratory (University of Chicago, Chicago, IL). LC-ESI-MS/MS chromatograms were acquired in MRM mode by monitoring transition pairs of 5mdC and 5hmdC.

2.10. Intracellular metabolite analysis

Assessment of intracellular metabolites was performed as previously described [17,18]. Briefly, cells were lysed in 100% methanol and frozen at -80 °C prior to centrifugation and collection of supernatants. Supernatants were then dried using a speedvac. Metabolites were analyzed with LC-MS/MS using the selected reaction monitoring (SRM) method with positive/negative ion polarity switching on a Xevo TQ-S mass spectrometer. Peak areas were integrated using MassLynx 4.1 (Waters Inc.) and were normalized to the respective cell count. Resultant peak areas were subjected to relative quantification analyses by utilizing Metaboanalyst 3.0.

2.11. Statistics

Data are presented as mean ± standard error of the mean (SEM) with N values displayed using individual markers. For two group comparison, significance was assessed using the Mann-Whitney U test or the Student's t-test dependent upon parametric distribution. For multiple group comparison, significance was assessed using a 2-way ANOVA followed by Bonferroni post-hoc analysis. Differences were considered significant at p < 0.05.

3. Results

3.1. MnSOD loss specifically increases steady-state mitochondrial O₂^{•-} in T-lymphocytes

Constitutive MnSOD knock-out mice are lethal early after birth and our previous report demonstrated significant T-lymphocyte developmental issues in T-lymphocyte-specific MnSOD knock-out animals [10,19], which limited any examination of these cells in a fully developed adult model. To address this limitation, we developed a novel inducible MnSOD knock-out mouse by crossing MnSOD floxed mice to mice expressing a tamoxifen-inducible estrogen receptor/cre

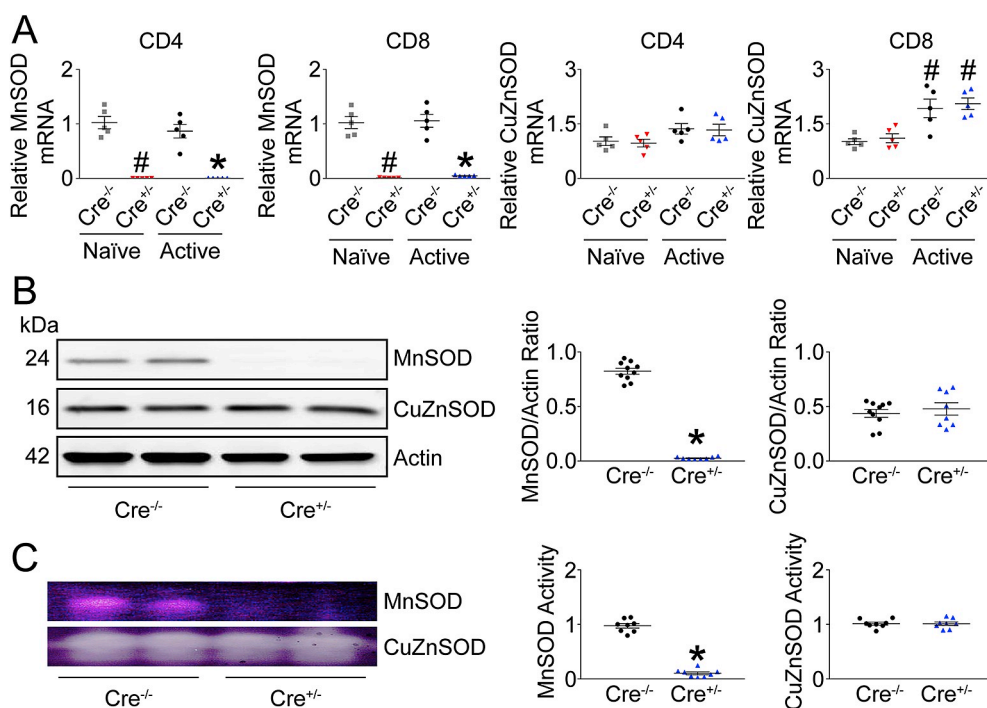


Fig. 1. MnSOD in T-lymphocytes is efficiently removed using an inducible knock-out strategy. Tamoxifen was administered to MnSOD knock-out (Cre^{+/-}) and control (Cre^{-/-}) mice for five consecutive days followed by two weeks to allow full recombination and loss of MnSOD. Splenic T-lymphocytes were isolated from mice and analyzed in either their naïve or activated (cultured with anti-CD3 and anti-CD28 beads for 96 h) states. **A. Left**, MnSOD gene and **right**, CuZnSOD gene mRNA levels assessed by quantitative real-time RT-PCR. **B. Left**, representative western blot of MnSOD and CuZnSOD. **Right**, quantification of respective proteins. **#p** < 0.01 versus naïve Cre^{-/-}; ***p** < 0.01 versus activated Cre^{-/-} by parametric Student's *t*-test or nonparametric Mann-Whitney *U* test where appropriate.

recombinase fusion protein under the control of the ROSA26 promoter [11]. This promoter was chosen due its ubiquitous expression in both CD4⁺ and CD8⁺ T-lymphocytes, as well as the availability of a tamoxifen-inducible cre recombinase model at the initiation of these studies. In contrast to our developmental model, we observed no differences in circulating or splenic T-lymphocyte numbers or subtype percentages after MnSOD knock-out (data not shown). MnSOD knock-out was confirmed by nearly non-detectable MnSOD mRNA levels in both CD4⁺ and CD8⁺ T-lymphocytes independent of activation status (naïve cells were activated for 96 h *ex vivo* by the addition of anti-CD3 and anti-CD28 coated beads; Fig. 1A). Loss of MnSOD did not induce any concomitant increases in transcripts for the nuclear/cytoplasmic/inner mitochondrial space-localized copper/zinc superoxide dismutase (CuZnSOD; encoded by the Sod1 gene), even though induction of this gene was observed in CD8⁺ cells upon activation (Fig. 1A). Loss of MnSOD was further confirmed at the protein and activity levels in pan-T-lymphocytes (due to the protein quantity requirements of these assays) without any change in CuZnSOD protein or activity compared to controls (Fig. 1B–C).

Electron paramagnetic resonance (EPR) assessment of MnSOD knock-out T-lymphocytes demonstrated significantly elevated intracellular O₂⁻ levels in both CD4⁺ and CD8⁺ cells (Fig. 2A). This was further confirmed by flow cytometry using the O₂⁻-sensitive fluorescent probe dihydroethidium (DHE; Fig. 2B). Both of these methodologies lack subcellular localization specificity, thus, the mitochondrial-targeted O₂⁻-sensitive fluorescent probe MitoSOX Red was utilized to identify specifically the mitochondrial redox environment. Using flow cytometry, assessment of MitoSOX Red oxidation confirmed an approximate 2-fold increase in steady-state mitochondrial O₂⁻ in both CD4⁺ and CD8⁺ MnSOD knock-out T-lymphocytes compared to controls (Fig. 2C). Increases in DHE and MitoSOX Red oxidation in naïve CD4⁺ and CD8⁺ MnSOD knock-out T-lymphocytes were comparable to their activated counterparts (data not shown). In contrast, the use of boronate-based fluorescent probes (*i.e.* PY1 and MitoPY1) that are sensitive to hydrogen peroxide (H₂O₂) and peroxynitrite (ONOO⁻) yielded no changes in oxidation (Fig. 2D–E). In summary, inducible loss of MnSOD significantly and specifically increases steady-state mitochondrial O₂⁻ in both CD4⁺ and CD8⁺ T-lymphocytes without compensation by CuZnSOD or a loss of cellularity *in vivo*.

3.2. Uncontrolled mitochondrial O₂⁻ severely disrupts T-lymphocyte cellular metabolism

Glycolytic and mitochondrial metabolism are critical regulators of T-lymphocyte activation, proliferation, and function [6], but it remains unknown how ROS like O₂⁻ affect these metabolic processes in T-lymphocytes. Using a Seahorse Bioanalyzer, we assessed oxygen consumption rate (OCR) and extracellular acidification rate (ECAR) in naïve and activated CD4⁺ and CD8⁺ T-lymphocytes under various metabolic states. Intriguingly, naïve MnSOD knock-out T-lymphocytes demonstrated few changes in glycolytic and mitochondrial metabolism under an elevated mitochondrial O₂⁻ environment, with maximal mitochondrial respiration rate, spare respiratory capacity, and proton leak being significantly affected compared to controls (Fig. 3A–B, Supplemental Fig. 1A). Upon activation of control T-lymphocytes, both glycolytic and mitochondrial metabolism increased significantly compared to naïve cells, as has been previously reported [8,20], however, MnSOD knock-out T-lymphocytes showed markedly transformed metabolic profiles. Activated CD4⁺ MnSOD knock-out cells exhibited nearly zero OCR at baseline as well as with oligomycin, FCCP, and rotenone/antimycin A challenges (Fig. 3A). Spare respiratory capacities and proton leak were also significantly affected in both CD4⁺ and CD8⁺ MnSOD knock-out cells (Supplemental Fig. 1A). In contrast, activated CD8⁺ MnSOD knock-out T-lymphocytes appeared more robust than their CD4⁺ counterparts showing an OCR profile similar to the naïve state of the cells (Fig. 3A). Glycolytic assessment of activated CD4⁺ MnSOD knock-out cells demonstrated no change at baseline, but decreased glycolytic capacity when challenged with glucose and oligomycin (Fig. 3B). Similarly, activated CD8⁺ MnSOD knock-out T-lymphocytes showed an even greater reduction in glycolytic capacity even at baseline (Fig. 3B). Both CD4⁺ and CD8⁺ activated MnSOD knock-out T-lymphocytes demonstrated completely absent glycolytic reserves (Supplemental Fig. 1B). Together, these data suggest endogenously produced, uncontrolled mitochondrial O₂⁻ has broad-reaching implications that dramatically affect cellular metabolic states differentially in CD4⁺ and CD8⁺ T-lymphocytes.

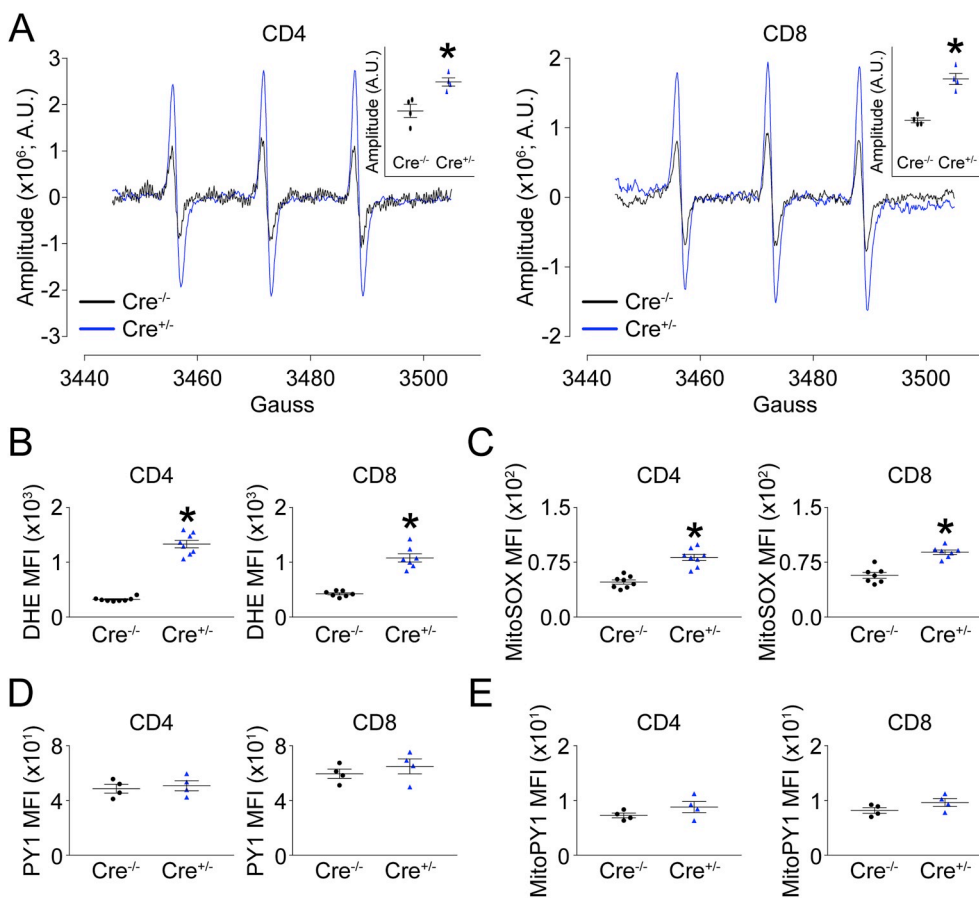


Fig. 2. Loss of MnSOD specifically increases steady-state $O_2^{\bullet-}$ in T-lymphocytes. Tamoxifen was administered to MnSOD knock-out ($Cre^{+/-}$) and control ($Cre^{-/-}$) mice for five consecutive days followed by two weeks to allow full recombination and loss of MnSOD. Splenic T-lymphocytes were isolated from mice activated by anti-CD3 and anti-CD28 beads in culture for 96 h. A. Representative electron paramagnetic resonance spectrums from $Cre^{-/-}$ and $Cre^{+/-}$ mice. Quantification located in inset. Also, flow cytometric fluorescent quantification of dihydroethidium staining (DHE) for total cellular $O_2^{\bullet-}$ (B), MitoSOX Red staining for mitochondrial $O_2^{\bullet-}$ (C), PY1 staining for total cellular H_2O_2 and $ONOO^-$ (D), and MitoPY1 staining for mitochondrial H_2O_2 and $ONOO^-$ (E). * $p < 0.01$ versus activated $Cre^{-/-}$ by parametric Student's t-test or nonparametric Mann-Whitney U test where appropriate.

3.3. Loss of MnSOD enhances T-lymphocyte proliferative gene expression while increasing apoptosis

Understanding the metabolic state of MnSOD knock-out T-lymphocytes appeared significantly dysregulated, we next assessed the ability of these cells to proliferate *ex vivo*. Control T-lymphocytes demonstrated characteristic growth curves with rapid expansion occurring between 48 and 96 h, and with $CD8^+$ cells proliferating faster than $CD4^+$ T-lymphocytes (Fig. 4A). MnSOD knock-out T-lymphocytes had significantly fewer cell numbers at later time points in both $CD4^+$ and $CD8^+$ T-lymphocytes, and this correlated with an amplified apoptotic fraction as assessed by increased annexin V and propidium iodide staining at 96 h post-activation (Fig. 4A–B). These findings confirmed our previous report of MnSOD loss causing increased apoptosis and a loss of cellularity in developing thymocytes [10]. To assess if the loss of MnSOD also disrupted normal cellular growth kinetics, we first assessed proliferation by carboxyfluorescein succinimidyl ester (CFSE) staining. To our surprise, MnSOD knock-out T-lymphocytes presented with no changes in proliferative indices (Fig. 4C). This observation was confirmed by an intracellular propidium iodide cell cycle analysis (Fig. 4D). Furthermore, as expected, analysis of regulatory cell cycle gene expression showed activated T-lymphocytes expressed higher levels of most pro-growth genes compared to naïve cells from control animals (Fig. 4E). Activated MnSOD knock-out T-lymphocytes demonstrated similar or higher expression of these genes compared to their activated counterparts (Fig. 4E), supporting our previous findings of normal proliferation. Interestingly, naïve knock-out T-lymphocytes expressed markedly significantly elevated levels of these genes compared to their naïve counterparts, and their profiles mimicked that of activated T-lymphocytes (Fig. 4E). However, these cells were unable to expand in culture without the addition of an activating stimulus (data not shown). These data suggest increased mitochondrial $O_2^{\bullet-}$ appears to

increase the proliferative capacity of T-lymphocytes, but is unable to successfully complete this process likely due to increased apoptosis and dysregulated metabolism.

3.4. Mitochondrial $O_2^{\bullet-}$ leads to global cytokine dysregulation in T-lymphocytes

In addition to proliferation, another hallmark of T-lymphocyte activation is cytokine and chemokine production. Activated $CD4^+$ MnSOD knock-out T-lymphocytes expressed the same or higher levels of interleukin 2 (IL-2), IL-4, IL-6, IL-10, IL-12, IL-17A, tumor necrosis factor alpha (TNF α), interferon gamma (IFN γ), C-C motif chemokine ligand 2 (CCL2), and CCL4 compared to controls (Fig. 5A–J). These cells also showed significant increases in IL-16, IL-27, and C-X-C motif chemokine 10 (CXCL10) with the only significant decrease being in IL-9 (data not shown). $CD8^+$ T-lymphocytes, in general, express different patterns of cytokine expression compared to $CD4^+$ cells, but MnSOD knock-out led to similar increases in most cytokines and chemokines assessed (Fig. 5A–J). In contrast to $CD4^+$ T-lymphocytes, $CD8^+$ MnSOD knock-out T-lymphocytes showed decreases in IL-10 and TNF α (Fig. 5D,G). These cells also showed significant increases in IL-16, IL-17C, IL-27, CXCL1, CXCL2, and CXCL10 with significant decreases being in IL-13 and IL-17F (data not shown). IL-1 β , IL-5, IL-17E, IL-21, IL-22, IL-31, IL-33, CCL3, and CCL20 were not significantly changed in either $CD4^+$ or $CD8^+$ MnSOD knock-out T-lymphocytes (data not shown). Together, these data suggest mitochondrial $O_2^{\bullet-}$ causes a global disruption of normal cytokine production in T-lymphocytes with no apparent predilection towards a specific polarization subtype.

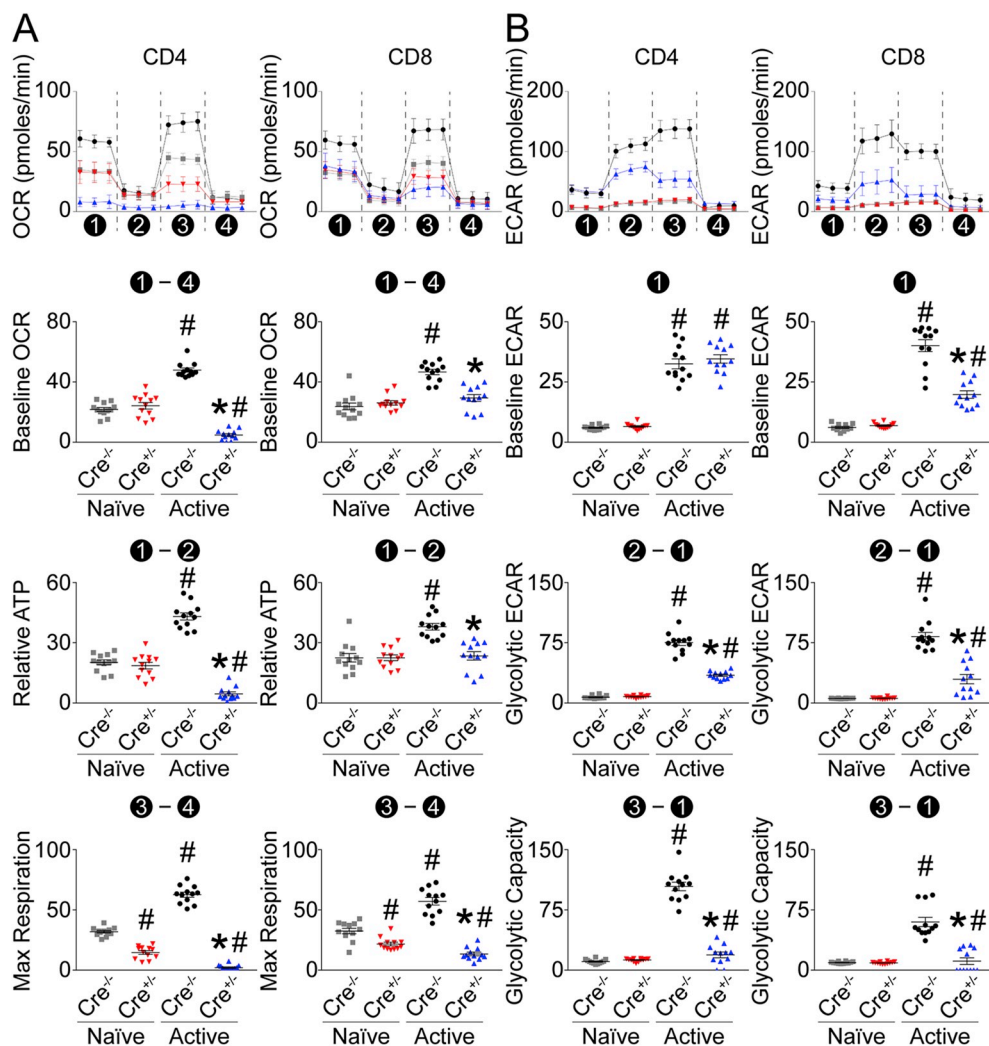


Fig. 3. Mitochondrial $O_2^{\bullet-}$ disrupts mitochondrial and glycolytic metabolism in T-lymphocytes. Tamoxifen was administered to MnSOD knock-out ($Cre^{-/-}$) and control ($Cre^{+/+}$) mice for five consecutive days followed by two weeks to allow full recombination and loss of MnSOD. Splenic T-lymphocytes were isolated from mice and analyzed in either their naïve or activated (cultured with anti-CD3 and anti-CD28 beads for 96 h) states. **A. Upper**, representative oxygen consumption rate (OCR) curves of a mitochondrial stress test. Colored lines correspond to color coding in quantifications below. **Lower**, quantification of metabolic states. Numbers correspond to respective time points or calculations on representative curves above. **B. Upper**, representative extracellular acidification rate (ECAR) curves of a glycolysis stress test. Colored lines correspond to color coding in quantifications below. **Lower**, quantification of metabolic states. Numbers correspond to respective time points or calculations on representative curves above. # $p < 0.01$ versus naïve $Cre^{-/-}$; * $p < 0.01$ versus activated $Cre^{-/-}$ by 2-way ANOVA with multiple comparisons and Bonferroni post-hoc analysis.

3.5. DNA methylation and methionine metabolism are disrupted by MnSOD loss

Gene expression analysis of MnSOD knock-out T-lymphocytes demonstrated widespread dysregulation (Figs. 4–5), which suggested the potential for epigenetic processes being affected by uncontrolled mitochondrial $O_2^{\bullet-}$. We first examined global DNA cytosine methylation and hydroxymethylation in naïve $CD4^+$ and $CD8^+$ T-lymphocytes. The loss of MnSOD did not appear to change total amounts of these regulatory marks in naïve cells even with increases in mitochondrial $O_2^{\bullet-}$ levels (Fig. 6A). In contrast, total DNA methylation was decreased in both activated $CD4^+$ and $CD8^+$ MnSOD knock-out T-lymphocytes with concurrent increases in hydroxymethylation (Fig. 6B). Cytosine hydroxymethylation often occurs during active DNA demethylation, and is carried out by a class of enzymes known as the ten-eleven translocation methylcytosine dioxygenases (TET). Gene expression level of the TET enzymes was unchanged (Fig. 6C), which suggested DNA methylation may be affected by a mechanism other than increased expression of these regulatory proteins. S-adenosyl methionine (SAME) is the methyl donor for DNA methylation, and SAME's metabolism is tightly linked with the methionine cycle (Fig. 6D). Performing targeted intracellular metabolomics analysis, we observed that MnSOD loss in both $CD4^+$ and $CD8^+$ T-lymphocytes caused significant disruption in numerous metabolites involved in this pathway (Fig. 6E–J). Overall, our data suggest mitochondrial $O_2^{\bullet-}$ alters global cellular DNA methylation and hydroxymethylation in activated T-lymphocytes potentially through perturbations in intracellular metabolite pools, and this may be

one mechanism by which gene expression is dysregulated in these cells.

4. Discussion

For decades, the misuse of the term of “oxidative stress” has plagued the literature painting reactions with ROS as purely stressful or damaging, while limiting the essential role these species play in normal cellular physiology. Recently, the concept of redox signaling has become more widely accepted, and significant progress has been made in the understanding of how the redox environment shapes cellular function. However, investigations of redox signaling in T-lymphocytes are still in their infancy, and mostly have relied on examining cellular effects in the presence of non-physiological levels of exogenous oxidants. For example, several studies have shown that exogenous oxidants inhibit T-lymphocyte activation, and that supplementation with various antioxidants can reverse these effects [21–23]. Additional studies have shown that different T-lymphocyte subtypes also possess differential responses to exogenous oxidants [22,24,25]. To address the role of endogenous ROS on T-lymphocyte physiology, many investigators have utilized the strategy of pro-oxidant enzyme knock-out animals. Early work using this strategy identified that T-lymphocytes generated their own oxidants during activation, and that these ROS were critical in the proper cellular response [3,26]. These oxidants appeared to be produced primarily through NADPH oxidase 2 (Nox2) and possibly lipoxigenase [27–30]. Interestingly, the loss of Nox2 (and thus decreased production of cytoplasmic $O_2^{\bullet-}$) had significant impacts on T-lymphocyte polarization leading to a predominant T_H17 as opposed to the

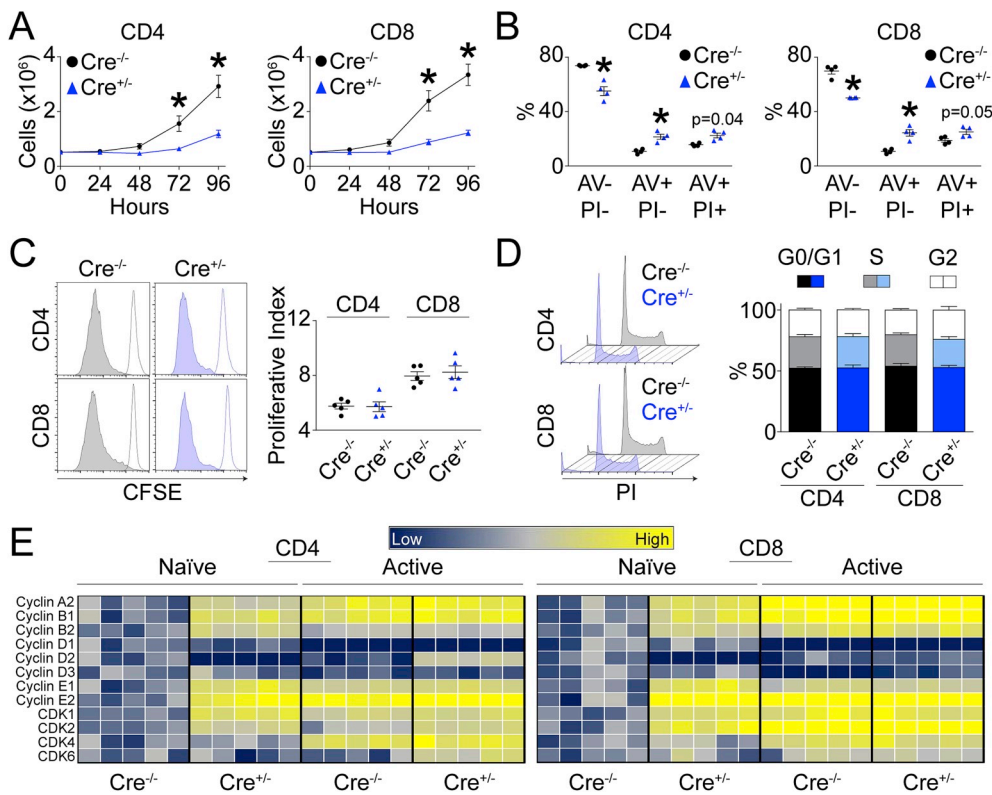


Fig. 4. Loss of MnSOD increases T-lymphocyte apoptosis while increasing proliferative capacity. Tamoxifen was administered to MnSOD knock-out (Cre^{-/-}) and control (Cre^{+/-}) mice for five consecutive days followed by two weeks to allow full recombination and loss of MnSOD. Splenic T-lymphocytes were isolated from mice and analyzed in either their naïve or activated (cultured with anti-CD3 and anti-CD28 beads for 96 h) states. **A.** Growth curves of T-lymphocytes at various time points. N = 6. **B.** Flow cytometric quantification of apoptotic fraction by annexin V (AV) and propidium iodide (PI) staining. AV-/PI- indicates healthy, viable cells; AV+/PI- indicates early apoptotic cells; AV+/PI+ indicates late apoptotic/necrotic cells. **C.** Flow cytometric quantification of CFSE staining. Open histogram represents cells stained pre-activation, while shaded histogram shows cells after 96 h of activation. Y-axis set to modal view for comparison. **D.** Flow cytometric quantification of the cell cycle utilizing intracellular propidium iodide staining. N = 6. **E.** Heat map representation of quantitative real-time RT-PCR analysis of various cell cycle genes. Each individual square represents one biological replicate. N = 5. *p < 0.01 versus activated Cre^{-/-} by parametric Student's t-test, nonparametric Mann-Whitney U test, or 2-way ANOVA with Bonferroni post-hoc analysis where appropriate.

characteristic T_H1 phenotype [29]. This is in contrast to our findings here that suggest increased mitochondrial O₂^{-•} leads to increased expression of all classically-defined subtype-specific cytokines (*i.e.* IFN γ , IL-17A, and IL-4). Furthermore, Nox-derived ROS have also been implicated in regulatory T-lymphocyte (T_{Reg}) polarization and function [31], but we did not observe any change in this specific subtype of cells (data not shown). Together, these studies and ours have begun to uncover specific regulatory functions of ROS, but many questions regarding specific mechanisms, subcellular locations, and the boundary between signaling and stress remains unresolved.

One major confounder in any study that perturbs cellular SOD levels is the impact this may have on steady state H₂O₂ levels. Because SOD converts O₂^{-•} to H₂O₂ at essentially diffusion-limited rates, it is enticing to assume that elimination or over-expression of this enzyme would therefore impact both levels of both species. However, in a complex and highly dynamic cellular system this is not always the case. Irwin Fridovich, the co-discoverer of SOD, has eloquently discussed this phenomenon recently, and explains that perturbation of SOD may increase, decrease, or not change H₂O₂ levels dependent upon cellular conditions [32]. In brief, while SOD does in fact increase the rate of H₂O₂ formation, its steady-state level is also highly reliant upon the presence and activity of H₂O₂ scavenging systems. We previously performed microarray analyses on MnSOD-deficient T-lymphocytes, and observed no expression changes of any H₂O₂ scavenging enzymes [10]. Additionally, our previous work showed MnSOD knock-out did not change DCFH-DA oxidation or nitrotyrosine levels [10], thus, taken into account with the absence of change in PY1 and MitoPY1 oxidation in the work presented here, these data are highly suggestive of no alterations in either H₂O₂ or ONOO⁻ steady-state levels with MnSOD loss. Given that we only utilized the boronate probes in this work, there is the slight possibility that these two oxidants are inversely dysregulated leading to no difference in overall oxidation of PY1 or MitoPY1.

We did attempt to utilize the roGFP and HyPer constructs as an additional method of O₂^{-•} and H₂O₂ measurement, but due to the fact that primary T-lymphocytes are highly resistant to transfection or transduction these attempts were unsuccessful. Future work crossing MnSOD knock-out animals with transgenic animals expressing these redox-sensitive fluorescent proteins will aid in the further elucidation of how MnSOD perturbation affects the cellular ROS environment.

The specific role of mitochondria ROS in T-lymphocyte function has been particularly elusive. Very few studies have attempted to resolve this question, but each has contributed insight into this organelle's contribution to redox signaling. By using inhibitors of complex I of the electron transport chain, Kaminski et al. suggested a role for mitochondrial-derived ROS in the production of IL-2 and IL-4 in T-lymphocytes [9], which correlates with our findings here. This same group also described a role for mitochondrial ROS in activation-induced cell death in mitochondrial depleted cells [33]. A more recent study investigated the role of complex III-derived ROS in T-lymphocyte function. Using T-lymphocyte-specific complex III subunit knock-out mice, Sena et al. showed both CD4⁺ and CD8⁺ T-lymphocyte proliferation and function was dependent upon ROS produced from this complex, and that attenuation of this ROS disrupted these processes [8]. Complex III is able to uniquely produce extra-mitochondrial O₂^{-•}, which the authors imply is how this specific ROS regulates cellular function. We demonstrate a similar dysregulated phenotype with increased mitochondrial O₂^{-•}, which again supports a proper balance of mitochondrial ROS are necessary for normal physiology of these cells. However, these previous studies utilizing electron transport chain perturbations to study the effects of mitochondrial ROS could be alternatively interpreted as alterations due solely to the cellular metabolic state. To address this, we developed a model of specific elevations in mitochondrial O₂^{-•} levels by targeting MnSOD. In this model, the likely source of O₂^{-•} is the electron transport chain (ETC), however, there are in fact other

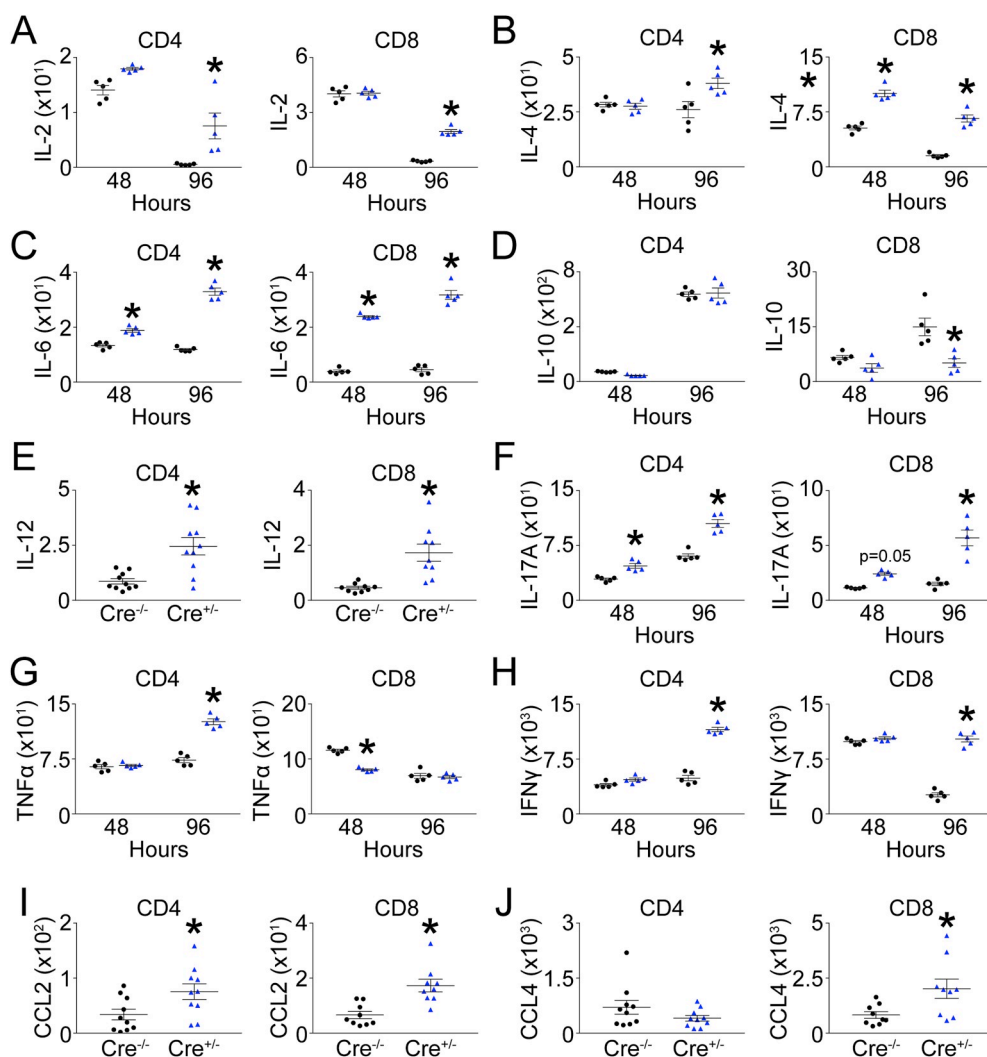


Fig. 5. Global cytokine and chemokine dysregulation occurs with increased steady-state mitochondrial $O_2^{\cdot-}$ in T-lymphocytes. Tamoxifen was administered to MnSOD knock-out ($Cre^{+/+}$) and control ($Cre^{-/-}$) mice for five consecutive days followed by two weeks to allow full recombination and loss of MnSOD. Splenic T-lymphocytes were isolated from mice activated by anti-CD3 and anti-CD28 beads in culture. Culture media was utilized for cytokine and chemokine analysis. **A, B, C, D, F, G, H.** Cytometric bead array analysis of various secreted cytokines at 48 and 96 h post-activation. **E, I, J.** Mesoscale multiplex array of various cytokines and chemokines at 96 h post-activation. Black circles indicate $Cre^{-/-}$, while blue triangles indicate $Cre^{+/+}$. Data are shown normalized to cell number at the respective time points. * $p < 0.01$ versus activated $Cre^{-/-}$ by parametric Student's *t*-test, nonparametric Mann-Whitney *U* test, or 2-way ANOVA with Bonferroni post-hoc analysis where appropriate.

sources of mitochondrial superoxide including the mitochondrial permeability transition pore as well as even NADPH oxidase isoforms [14,34]. It may be possible that the loss of MnSOD initially increases steady-state $O_2^{\cdot-}$ from the ETC, but chronically this ROS triggers other ROS generating systems as has been seen in other model systems [35]. Using this model, we previously showed a critical role for mitochondrial $O_2^{\cdot-}$ in T-lymphocyte development [10], but this deficit precluded this model from the examination of cellular function in fully mature lymphocytes. Herein, using this same mouse but with a novel inducible-strategy of MnSOD knock-out, we demonstrate that endogenously produced mitochondrial $O_2^{\cdot-}$ has broad-reaching and subtype-specific inflammatory, apoptotic, and epigenetic effects on $CD4^+$ and $CD8^+$ T-lymphocytes that appears driven at least in part by the dysregulation of cellular metabolism and metabolite pools. While in this work we did not directly examine the causal link between mitochondrial $O_2^{\cdot-}$ and our phenotypic changes, our previous studies have shown that the addition of mitochondrial $O_2^{\cdot-}$ scavengers to MnSOD knock-out immune cells was sufficiently able to reverse the effects of MnSOD loss [10,36]. This suggests mitochondrial $O_2^{\cdot-}$ is in fact the causal source behind the phenotypic changes, but more work is needed to identify the specific downstream proteins and pathways directly affected by this increased ROS. In any event, these findings strengthen the hypothesis that the mitochondrial redox environment is significantly coupled to metabolism, which suggests investigations into one of these physiological processes should inherently and necessarily involve examination of the other.

Metabolism is a primary regulator of T-lymphocytes, and the metabolic state has been shown to change dynamically dependent upon activation and polarization state of these cells [6]. Naïve T-lymphocytes reside in a metabolically quiescent state that is reliant upon mitochondrial oxidative phosphorylation as its predominant ATP source, whereas activated effector T-lymphocytes are mainly glycolytic. While this glycolytic shift, known as the Warburg effect, has been described in other rapidly dividing cells like cancer, the notion of glycolysis exclusively supporting cellular metabolism in proliferative cells is waning from popular view [37]. This is due to emerging evidence in both the immune and cancer fields that even though glycolytic rates significantly increase in proliferating cells, so do mitochondrial metabolic processes. For example, memory T-lymphocytes rely more on mitochondrial metabolism and even possess intricate mitochondrial network structures, which is believed to provide these cells with a specific replicative advantage upon antigenic challenge [38]. Additionally, elimination of glutamine, which is specifically metabolized in the mitochondria, prohibits T-lymphocytes from proper activation and proliferation [8]. Furthermore, loss of the hypoxia inducible factor 1 alpha (HIF1 α), which would lead to enhanced mitochondrial metabolism, alters T-lymphocyte polarization and cytokine production [39]. Our results confirm and extend the importance of the mitochondria to T-lymphocytes by demonstrating that disruption of oxidative metabolism by increased $O_2^{\cdot-}$ has far-reaching consequences on the ability of these cells to properly activate. In fact, loss of MnSOD actually increased pro-growth gene expression (possibly a compensatory mechanism due to

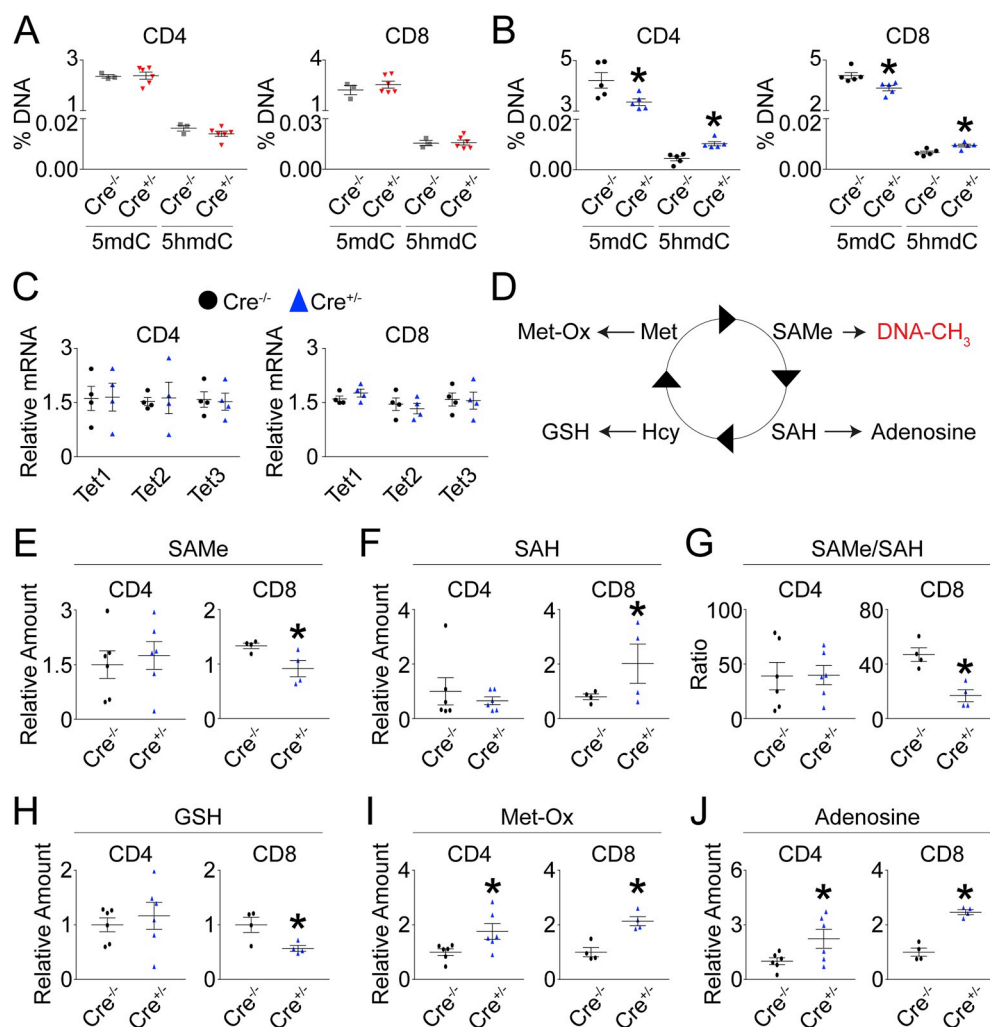


Fig. 6. Elevated mitochondrial $O_2^{\bullet-}$ disrupts the T-lymphocyte metabolic-epigenetic axis. Tamoxifen was administered to MnSOD knock-out ($Cre^{+/+}$) and control ($Cre^{-/-}$) mice for five consecutive days followed by two weeks to allow full recombination and loss of MnSOD. Splenic T-lymphocytes were isolated from mice and analyzed in either their naïve or activated (cultured with anti-CD3 and anti-CD28 beads for 96 h) states. **A.** Global DNA cytosine methylation (5mdC) and hydroxymethylation (5hmdC) shown as percent of total nucleotides in naïve T-lymphocytes. **B.** Global DNA cytosine methylation (5mdC) and hydroxymethylation (5hmdC) shown as percent of total nucleotides in activated T-lymphocytes. **C.** TET gene mRNA levels as assessed by quantitative real-time RT-PCR. **D.** Schematic of the methionine cycle in reference to DNA methylation. Targeted intracellular metabolomics analysis of S-adenosyl methionine (SAME; **E**), S-adenosyl homocysteine (SAH; **F**), SAME/SAH ratio (**G**), total glutathione (GSH; **H**), methionine sulfoxide (Met-Ox; **I**), and adenosine (**J**). * $p < 0.01$ versus activated $Cre^{-/-}$ by parametric Student's t-test, nonparametric Mann-Whitney U test, or 2-way ANOVA with Bonferroni post-hoc analysis where appropriate.

increased apoptosis), but even with the high abundance of these genes the cells were not able to proliferate more readily than wild-type cells. We hypothesize this may be due to the global disruption of metabolism hindering the proliferative abilities of these T-lymphocytes. Furthermore, it has been previously observed that $CD4^+$ effector T-lymphocytes rely on oxidative metabolism more than $CD8^+$ cells [40], which may suggest the differential metabolic profiles we observed in our model. These metabolic differences may also explain the variations in metabolite pools in $CD4^+$ and $CD8^+$ cells with increased mitochondrial $O_2^{\bullet-}$, which likely impacts the epigenetic landscape of the cells. However, the exact mechanisms underlying the redox, metabolic, and epigenetic control of the T-lymphocytes warrant further investigation.

The epigenome is the next frontier of human genetics. Unlike the genome that utilizes primarily four nucleotides in its code, the epigenome utilizes a vast assortment of processes to regulate gene expression. These include DNA methylation and hydroxymethylation, RNA methylation and hydroxymethylation, various histone modifications, chromatin accessibility, microRNA, and many more, and all of these processes have been reported to be at least partially redox-regulated [41]. For example, the TET enzymes and Jumonji C-domain-containing (JmjC) proteins that regulate DNA and histone demethylation, respectively, require α -ketoglutarate, molecular oxygen (O_2), and reduced iron to perform their catalytic functions. All of these co-factors are tightly associated with the redox and metabolic environments of the cell, suggesting intimate crosstalk between these processes. Indeed, oxygen availability and metabolite pools have previously been shown to regulate these enzymes [42–44]. We observed increased DNA

hydroxymethylation with concurrent decreased methylation in T-lymphocytes lacking MnSOD, yet, no changes in TET expression levels. While we propose the DNA methylation dysregulation is due to the decrease in SAME levels and disruption of the methionine cycle with increased mitochondrial $O_2^{\bullet-}$, it could also be possible that the change in global epigenetic DNA modifications may be due to perturbations in the aforementioned enzyme cofactors affecting TET function as opposed to expression. Other common epigenetic modifications include acetylation, glutathionylation, and adenylation, which are also closely linked with the redox and metabolic environments of cells. We observed changes in global glutathione and adenosine pools in MnSOD knock-out T-lymphocytes suggesting these processes are likely also dysregulated, though further studies are needed to identify the specific contribution of each modification to the observed phenotype. Another possibility for the alterations in nuclear gene expression could be that simply redox-sensitive transcription factors are being activated or inactivated due to the increased mitochondrial redox environment. This is especially true in the naïve cells that demonstrated significant gene expression, but minimal to no changes in metabolism, metabolite pools, or epigenetic changes. While it is highly likely some or all of these processes are altered by the increase in mitochondrial $O_2^{\bullet-}$, it remains unlikely that this highly reactive free radical is traversing the cellular milieu to directly affect expression processes in the nucleus. Our data support a model of redox-sensitive intermediates (e.g. metabolites) that ultimately affect cellular transcription and other processes, and ongoing work in our laboratory is thoroughly examining this hypothesis.

In conclusion, our study provides the first evidence that endogenous

uncontrolled mitochondrial $O_2^{\cdot-}$ in T-lymphocytes disrupts cellular gene expression and epigenetic control likely through alterations of cellular metabolism and metabolite pools. The increased expression of cell cycle genes, inflammatory cytokines, as well as the viability (> 50%) of the cells suggests these levels of mitochondrial $O_2^{\cdot-}$ represent a boundary between redox-signaling and oxidative stress. Intriguingly, while many genes were dysregulated with the loss of MnSOD, numerous remained unchanged. It continues to be unknown how affecting global cellular metabolism and the total bioavailability of specific metabolites targets specific genes while sparing others. This may be due to specific epigenetic regulatory sites evolutionarily being located in close proximity to metabolically-linked genes, but this hypothesis has yet to be fully explored. Overall, this study provides new evidence of the importance and widespread impact of mitochondrial $O_2^{\cdot-}$ in cells of the adaptive immune system.

Author contributions

CMM, CWC, VG, AV, JZC, PKS, LAG, and AJC designed research studies; CMM, CWC, VG, AV, JZC, and AJC conducted experiments and acquired/analyzed data; PKS, LAG, and AJC provided reagents and performed experimental oversight; AJC wrote the manuscript.

Conflicts of interest

The authors have declared that no conflict of interest exists.

Acknowledgments

This work was supported by NIH R00HL123471 to AJC. We thank Dr. Matthew Zimmerman, University of Nebraska Medical Center, for his assistance with this work.

Appendix A. Supplementary data

Supplementary data to this article can be found online at <https://doi.org/10.1016/j.redox.2019.101141>.

References

- A.J. Case, On the origin of superoxide dismutase: an evolutionary perspective of superoxide-mediated redox signaling, *Antioxidants (Basel)* 6 (4) (2017), <https://doi.org/10.3390/antiox6040082>.
- M. Schieber, N.S. Chandel, ROS function in redox signaling and oxidative stress, *Curr. Biol.* 24 (2014) R453–R462.
- S.H. Jackson, S. Devadas, J. Kwon, L.A. Pinto, M.S. Williams, T cells express a phagocyte-type NADPH oxidase that is activated after T cell receptor stimulation, *Nat. Immunol.* 5 (2004) 818–827.
- P. Kesarwani, A.K. Murali, A.A. Al-Khami, S. Mehrotra, Redox regulation of T-cell function: from molecular mechanisms to significance in human health and disease, *Antioxidants Redox Signal.* 18 (12) (2013) 1497–1534.
- C.H. Chang, E.L. Pearce, Emerging concepts of T cell metabolism as a target of immunotherapy, *Nat. Immunol.* 17 (4) (2016) 364–368.
- E.L. Pearce, M.C. Poffenberger, C.H. Chang, R.G. Jones, Fueling immunity: insights into metabolism and lymphocyte function, *Science* 342 (2013) 1242–1245.
- M.D. Buck, D. O'Sullivan, E.L. Pearce, T cell metabolism drives immunity, *J. Exp. Med.* 212 (2015) 1345–1360.
- L.A. Sena, S. Li, A. Jairaman, et al., Mitochondria are required for antigen-specific T cell activation through reactive oxygen species signaling, *Immunity* 38 (2013) 225–236.
- M.M. Kaminski, S.W. Sauer, C.D. Klemke, et al., Mitochondrial reactive oxygen species control T cell activation by regulating IL-2 and IL-4 expression: mechanism of ciprofloxacin-mediated immunosuppression, *J. Immunol.* 184 (9) (2010) 4827–4841.
- A.J. Case, J.L. McGill, L.T. Tygrett, et al., Elevated mitochondrial superoxide disrupts normal T cell development, impairing adaptive immune responses to an influenza challenge, *Free Radic. Biol. Med.* 50 (2011) 448–458.
- A.J. Case, J. Tian, M.C. Zimmerman, Increased mitochondrial superoxide in the brain, but not periphery, sensitizes mice to angiotensin II-mediated hypertension, *Redox Biol.* 11 (2016) 82–90.
- A.J. Case, C.T. Roessner, J. Tian, M.C. Zimmerman, Mitochondrial superoxide signaling contributes to norepinephrine-mediated T-lymphocyte cytokine profiles, *PLoS One* 11 (10) (2016) e0164609.
- A.J. Case, M.C. Zimmerman, Redox-regulated suppression of splenic T-lymphocyte activation in a model of sympathoexcitation, *Hypertension* 65 (2015) 916–923.
- A.J. Case, S. Li, U. Basu, J. Tian, M.C. Zimmerman, Mitochondrial-localized NADPH oxidase 4 is a source of superoxide in angiotensin II-stimulated neurons, *Am. J. Physiol. Heart Circ. Physiol.* 305 (2013) H19–H28.
- A. Vasanthakumar, J.B. Lepore, M.H. Zegarek, et al., Dnm3b is a haploinsufficient tumor suppressor gene in myc-induced lymphomagenesis, *Blood* 121 (11) (2013) 2059–2063.
- L. Song, S.R. James, L. Kazim, A.R. Karpf, Specific method for the determination of genomic DNA methylation by liquid chromatography-electrospray ionization tandem mass spectrometry, *Anal. Chem.* 77 (2) (2005) 504–510.
- S.K. Shukla, V. Purohit, K. Mehla, et al., MUC1 and HIF-1 α signaling crosstalk induces anabolic glucose metabolism to impart gemcitabine resistance to pancreatic cancer, *Cancer Cell* 32 (1) (2017) 71–87 e7.
- V. Gunda, F. Yu, P.K. Singh, Validation of metabolic alterations in microscale cell culture lysates using hydrophilic interaction liquid chromatography (HILIC)-tandem mass spectrometry-based metabolomics, *PLoS One* 11 (4) (2016) e0154416.
- Y. Li, T.T. Huang, E.J. Carlson, et al., Dilated cardiomyopathy and neonatal lethality in mutant mice lacking manganese superoxide dismutase, *Nat. Genet.* 11 (1995) 376–381.
- C.H. Chang, J.D. Curtis, J. Maggi LB, et al., Posttranscriptional control of T cell effector function by aerobic glycolysis, *Cell* 153 (2013) 1239–1251.
- S. Gomerski, A. Cantagrel, J.P. Van Meerwijk, P. Romagnoli, Reactive oxygen species differentially affect T cell receptor-signaling pathways, *J. Biol. Chem.* 277 (22) (2002) 19585–19593.
- D. Mougialakos, C.C. Johansson, R. Kiessling, Naturally occurring regulatory T cells show reduced sensitivity toward oxidative stress-induced cell death, *Blood* 113 (15) (2009) 3542–3545.
- E. Flescher, J.A. Ledbetter, G.L. Schieven, et al., Longitudinal exposure of human T lymphocytes to weak oxidative stress suppresses transmembrane and nuclear signal transduction, *J. Immunol.* 153 (11) (1994) 4880–4889.
- A. Takahashi, M.G. Hanson, H.R. Norell, et al., Preferential cell death of CD8+ effector memory (CCR7-CD45RA-) T cells by hydrogen peroxide-induced oxidative stress, *J. Immunol.* 174 (10) (2005) 6080–6087.
- I. Bogeski, C. Kummerow, D. Al-Ansary, et al., Differential redox regulation of ORAI ion channels: a mechanism to tune cellular calcium signaling, *Sci. Signal.* 3 (115) (2010) ra24.
- S. Devadas, L. Zaritskaya, S.G. Rhee, L. Oberley, M.S. Williams, Discrete generation of superoxide and hydrogen peroxide by T cell receptor stimulation: selective regulation of mitogen-activated protein kinase activation and fas ligand expression, *J. Exp. Med.* 195 (2002) 59–70.
- M. Los, H. Schenk, K. Hexel, P.A. Baeuerle, W. Droge, K. Schulze-Osthoff, IL-2 gene expression and NF- κ B activation through CD28 requires reactive oxygen production by 5-lipoxygenase, *EMBO J.* 14 (15) (1995) 3731–3740.
- A.V. Belikov, B. Schraven, L. Simeoni, TCR-triggered extracellular superoxide production is not required for T-cell activation, *Cell Commun. Signal.* 12 (2014) 50-5014-0050-1.
- H.M. Tse, T.C. Thayer, C. Steele, et al., NADPH oxidase deficiency regulates th lineage commitment and modulates autoimmunity, *J. Immunol.* 185 (9) (2010) 5247–5258.
- R.D. Michalek, K.J. Nelson, B.C. Holbrook, et al., The requirement of reversible cysteine sulfenic acid formation for T cell activation and function, *J. Immunol.* 179 (10) (2007) 6456–6467.
- O. Efimova, P. Szankasi, T.W. Kelley, Ncf1 (p47phox) is essential for direct regulatory T cell mediated suppression of CD4+ effector T cells, *PLoS One* 6 (1) (2011) e16013.
- S.I. Liochev, I. Fridovich, The effects of superoxide dismutase on H₂O₂ formation, *Free Radic. Biol. Med.* 42 (10) (2007) 1465–1469.
- M. Kaminski, M. Kiessling, D. Suss, P.H. Krammer, K. Gulow, Novel role for mitochondria: protein kinase c θ -dependent oxidative signaling organelles in activation-induced T-cell death, *Mol. Cell Biol.* 27 (10) (2007) 3625–3639.
- H.A. Itani, A.E. Dikalova, W.G. McMaster, et al., Mitochondrial cyclophilin D in vascular oxidative stress and hypertension, *Hypertension* 67 (6) (2016) 1218–1227.
- S.I. Dikalov, R.R. Nazarewicz, A. Bikineyeva, et al., Nox2-induced production of mitochondrial superoxide in angiotensin II-mediated endothelial oxidative stress and hypertension, *Antioxidants Redox Signal.* 20 (2014) 281–294.
- A.J. Case, J.M. Madsen, D.G. Motto, D.K. Meyerholz, F.E. Domann, Manganese superoxide dismutase depletion in murine hematopoietic stem cells perturbs iron homeostasis, globin switching, and epigenetic control in erythrocyte precursor cells, *Free Radic. Biol. Med.* 56 (2013) 17–27.
- P.E. Porporato, N. Filigheddu, J.M.B. Pedro, G. Kroemer, L. Galluzzi, Mitochondrial metabolism and cancer, *Cell Res.* 28 (3) (2018) 265–280.
- G.J. van der Windt, D. O'Sullivan, B. Everts, et al., CD8 memory T cells have a bioenergetic advantage that underlies their rapid recall ability, *Proc. Natl. Acad. Sci. U. S. A.* 110 (35) (2013) 14336–14341.
- E.V. Dang, J. Barbi, H.Y. Yang, et al., Control of T(H)17/T(reg) balance by hypoxia-inducible factor 1, *Cell* 146 (5) (2011) 772–784.
- Y. Cao, J.C. Rathmell, A.N. Macintyre, Metabolic reprogramming towards aerobic glycolysis correlates with greater proliferative ability and resistance to metabolic inhibition in CD8 versus CD4 T cells, *PLoS One* 9 (8) (2014) e104104.
- A.R. Cyr, F.E. Domann, The redox basis of epigenetic modifications: from mechanisms to functional consequences, *Antioxidants Redox Signal.* 15 (2) (2011) 551–589.
- T. Laukka, C.J. Mariani, T. Ihtantola, et al., Fumarate and succinate regulate expression of hypoxia-inducible genes via TET enzymes, *J. Biol. Chem.* 291 (8) (2016) 4256–4265.
- C.J. Mariani, A. Vasanthakumar, J. Madzo, et al., TET1-mediated hydroxymethylation facilitates hypoxic gene induction in neuroblastoma, *Cell Rep.* 7 (5) (2014) 1343–1352.
- B. Thienpont, J. Steinbacher, H. Zhao, et al., Tumour hypoxia causes DNA hypermethylation by reducing TET activity, *Nature* 537 (7618) (2016) 63–68.